HHS Public Access

Author manuscript

*Biomacromolecules*. Author manuscript; available in PMC 2024 August 14.

Published in final edited form as:

*Biomacromolecules*. 2023 August 14; 24(8): 3638–3646. doi:10.1021/acs.biomac.3c00385.

# Antibody Polymer Conjugates (APCs) for Active Targeted Therapeutic Delivery

**Pintu Kanjilal**[1], **Khushboo Singh**[1], **Ritam Das**[1], **Joseph Matte**[1], **S. Thayumanavan**[1,2,3,4]

[1]Department of Chemistry, University of Massachusetts, Amherst, Massachusetts 01003, United States

[2]Department of Biomedical Engineering, University of Massachusetts, Amherst, Massachusetts 01003, United States

[3]Molecular and Cellular Biology Program, and University of Massachusetts, Amherst, Massachusetts 01003, United States

[4]The Center for Bioactive Delivery-Institute for Applied Life Sciences, University of Massachusetts, Amherst, Massachusetts 01003, United States

## Abstract

Antibody drug conjugates (ADCs) are poised to have enormous impact on targeted nanomedicine especially in many cancer pathologies. The reach of the current format of ADCs is limited by their low drug-to-antibody ratio (DAR), because of the associated physiochemical instabilities. Here, we design antibody polymer conjugates (APCs) as a modular strategy to utilize polymers to address ADC's shortcomings. We show here that conjugation of polymer-based therapeutic molecules to antibodies help increase the DAR, owing to the hydrophilic co-monomer in the polymer that helps in masking the increased hydrophobicity caused by high drug loading. We show that the platform exhibits cell targetability and selective cell killing in multiple cell lines expressing disease-relevant antigens, *viz.*, HER2 and EGFR. The ability to use different functionalities in the drug as the handle for polymer attachment further demonstrates the platform nature of APCs. The findings here could serve as an alternative design strategy for next generation of active targeted nanomedicine.

## Graphical Abstract

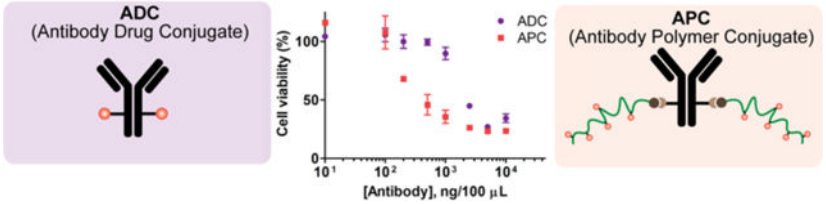


SUPPORTING INFORMATION

The supporting Information is available free of charge at pub.acs.org

Materials, a detailed synthetic protocol for monomer and polymers, characterization of monomer and polymers using $^{1}H$ NMR, $^{13}C$ NMR, gel permeation chromatography (GPC) as needed, supporting figures and tables.

**Keywords**

ADC; Kadcyla®; Active targeted delivery; Breast cancer; Antibody polymer conjugates

## INTRODUCTION

Antibody drug conjugates (ADCs) are one of the fastest growing class of therapeutics for targeted oncology treatments.[1–3] The FDA approval of 14 ADCs for hematological and solid tumor malignancies have demonstrated its potential in the clinical landscape and paved the way for many more ongoing clinical trials.[4,5] Typically, ADC constitutes a few chemotherapeutic molecules attached to a targeting antibody though a linker, where the antibody provides the specificity towards tumor-associated/tumor-specific cell surface antigens[6,7] The interest in ADCs as a targeted therapeutic approach originated with the approval of gemtuzumab ozogamicin (Mylotarg™) for the CD33-targeting treatment of acute myeloid leukemia.[8] While approvals of many more ADCs followed,[9] the potential of this platform has not been fully harnessed due to a few limitations;[10,11] chief among these involves the limited drug to antibody ratio (DAR). The original ADC, Mylotarg, had a DAR of ~2–3 and this number has not improved much beyond ~4 since that time, which in turn necessitates the use of highly potent drugs, thereby limiting the drug choices.[12] Limits on the DAR is attributed to hydrophobicity of payloads that lower the physiochemical stability of high DAR ADCs.[13,14] To address this, approaches that include the introduction of hydrophilic spacers such as PEG,[15–16] polysarcosine,[17] and macrocycles[18] have been shown to exhibit enhanced *in vivo* performance.[19] In this work, we present a monoclonal antibody-guided polymeric system, APC (antibody polymer conjugate), as a promising alternative approach to mitigate the shortcomings of the classical ADCs. In this design, a targeting antibody is attached to multiple copies of a random copolymer that is based on a combination of a hydrophilic PEG-containing monomer and a hydrophobic drug-containing monomer. Rather than using PEG moieties as spacer, we envisioned attaching a copolymer that contains the hydrophilic oligoethyleneglycol units (short PEG units) randomly distributed among drug-bearing monomers. Such a strategy would offer to mitigate the possibility of hydrophobic patches that render these conjugates physiochemically unstable, while offering the handles to incorporate multiple copies of the drug molecule from each conjugation site on the antibody (Figure 1). Using anti-HER2 antibody as the test case, we report here on the targetability and selective cell killing ability of the APCs *in vitro,* in comparison with the Kadcyla®, a drug in the clinic for treating HER2 overexpressing breast cancer.[21] To further demonstrate the broad applicability of this approach, we have also synthesized and tested the APC based on anti-EGFR (epidermal growth factor receptor), another target recognized for its therapeutic potential.[22]

## MATERIALS AND METHODS

### Monomer/Polymer Synthesis:

Detailed synthesis and characterization of pyridyl methacrylate monomer, BOC protected amino ethyl monomer, p-nitrophenyl carbonate monomer as well as polymer P1 (PEG-*co*-

PDS), polymer P2 (PEG-*co*-PDS-*co*-NHBOC), polymer P3 (PEG-*co*-NPC) are described in the Supporting Information.

### Antibody Modification with NHS-PEG8-DBCO linker:

Anti-HER2, anti-EGFR, anti-IgG antibodies were used in this study; same protocol was followed for linker conjugation across all antibodies. 500 μg of antibody was diluted in 500 μL reaction buffer composed of 0.2 M $Na_2HPO_4$ and 0.1 M NaCl at pH 8.5 and was buffer exchanged using 50 kDa Amicon ultracentrifugation filter. The solution was spun down to a final volume of 100 μL after repeating the exchange process two times at 4 °C. Afterwards, the solution was transferred to a 500 μL Eppendorf tube, NHS-PEG8-DBCO linker (in DMSO) was added to the antibody solution and incubated at 4 °C overnight. Two different linkers to antibody (LAR) were targeted for anti-HER2 antibody. For a target LAR of 2 and 5, 7X and 45X linker solution were added respectively. Finally, the unreacted linker was removed from the reaction mixture by centrifugation using 50 kDa Amicon ultracentrifugation filter. The LAR and antibody concentrations were assessed UV-vis spectroscopy absorbances at 280 nm and 310 nm.

### Drug Conjugations to Polymers:

For the DM1 drug conjugation to the polymer, 2 mg polymer P1 (PEG-*co*-PDS) was dissolved 1 mL DI water. To this, 0.5 or 1.0 equivalent of DM1 (DMSO, 10 mg/mL) stock solution were added and allowed to stir overnight. The drug equivalent was calculated with respect to the total moles of PDS in polymer P1 (by average MW). Then an aliquot of reaction volume was used to determine the moles of conjugated drug via UV-vis spectroscopy using the absorbance peak of 2-mercaptopyridine byproduct at 343 nm. The unreacted drug and the byproduct were dialyzed out using 2 mL 8 kDa mini dialysis kit against DI water for 24 h. For SN38 conjugation, 2 mg polymer P3 (PEG-*co*-NPC) was dissolved in 1 mL of DCM and added 1.0 equivalent of SN38 (DMSO, 10 mg/mL) stock solution. Followed by this, DMAP was added and allowed to stir overnight. Then the DCM was evaporated by gentle air purge to a minimum volume and 1 mL of water was added while continuous stirring. The solution was sonicated for a few minutes and then stirred for three hours at room temperature. The unreacted drug was dialyzed out using a 2 mL 8 kDa mini dialysis kit for 24 h.

### Preparation of APC:

The antibody-polymer conjugation was done in a 500 μL Eppendorf tube where antibody and polymers were incubated on shaker for 48 h at room temperature. We formulated three different APC systems for different purposes across this study. (i) Free polymer chain was conjugated to antibody for confirm the conjugation via SDA-PAGE and Western blot, flow cytometry binding evaluation via fluorophore tagged secondary antibody. (ii) fluorophore-(Sulfo-Cy3)-tagged polymer was conjugated to directly evaluate the binding interaction using flow cytometry. (iii) Drug-conjugated polymer to study cellular cytotoxicity. In all cases, same conjugation and purification protocol was followed. For conjugating polymer to antibody, 100 μg of linker conjugated antibody was taken in an Eppendorf followed by the addition of the polymer solution. Total reaction volume was made up to 100 μL by adding PBS. For lower or higher number of polymer chains per antibody, 20 equivalent of polymer

with respect to the linkers were added to the solution, respectively. Finally, the unreacted polymer was removed by centrifugation using 100 kDa Amicon ultracentrifugation filters. Disappearance of DBCO UV-vis absorbance peak at 310 nm, SDS-PAGE and Western blot were used as antibody polymer conjugation confirmation, and BCA assay was used to determine the antibody concentration after purification.

### SDS-PAGE gel run:

SDS-PAGE gel run was used to evaluate the antibody-polymer conjugation reaction and the smeared nature of band was considered as a confirmation of successful conjugations. For gel run, 5 μg of free antibody or antibody polymer conjugates were mixed with 10 μL gel loading buffer, which was then loaded into the acrylamide gel. The gel was run in 1X SDS running buffer at a constant voltage of 130 V for 1 h. The gel was stained in Coomassie stain solution for a few hours followed by destaining using 45% v/v methanol and 10% v/v acetic acid solution as needed. Finally, the gels were imaged and analyzed using Bio-Rad ChemiDoc imaging system.

### Western Blot:

We used Western blots as an additional antibody-polymer conjugation confirmation to the SDS-PGAE gel images. The protocol starts with SDS-PAGE gel run (above stated protocol) followed by the protein transfer to a polyvinylidene difluoride (PVDF) membrane at 100 V for 1 h in transfer buffer comprised of 25 mM Tris base, 0.192 M glycine, and 200 mL methanol. The membrane was blocked with 5% milk in 1X TBS Tween-20 for 1 h at room temperature followed by the incubation with HER2/ErbB2 primary antibody (1:1000 dilution in PBS) at 4 °C overnight. The membrane was washed with 0.1% Tween-20 for three times with a 15 min gentle shaking each time and incubation with secondary antibody for an hour at room temperature. Finally, the membrane was washed again with 0.1% Tween-20 in PBS, incubated with Bio-Rad's chemiluminescent and colorimetric detection kits, and imaged the membrane using Bio-Rad ChemiDoc imaging system.

### Flow Cytometry Studies:

Flow cytometry assay was used to evaluate the cellular binding of APC using i) secondary fluorophore-tagged antibody, ii) fluorophore-tagged polymer conjugated APC, and to quantify the receptor expression in different cell lines. We have used HER2+ (SKOV3, SKBR3, BT474), HER2- (MCF10A) cells and EGFR+ (A431) cells for our study and evaluated the binding interactions using secondary antibody in all these cells. For secondary antibody labelling method, 0.2 million cells in 100 μL media were taken in 500 μL Eppendorf tube, added 5 μg of antibody/APCs as needed and incubated for 30 minutes at 37 °C maintaining 5% $CO_2$. The cells were washed two times with cold PBS and incubated with APC labelled secondary antibody following suggested protocol. Cells were washed again with PBS and resuspended in FACS buffer flow cytometry analysis. A binding study using fluorophore-tagged APC was done in SKOV3 and MCF10A cells. The same protocol was followed here except for the incubation with fluorophore tagged secondary antibody. After 30 min of incubations, cells were washed with PBS, resuspended in FACS buffer for flow assay. To quantify the receptor expression, 0.2 million cells were taken in 500 μL Eppendorf, incubated with fluorophore tagged HER2 or EGFR primary antibody, as needed,

washed with PBS and resuspended them in FACS buffer for flow assay. The samples were run on BD LSRFortessa using FACSDiva software and data was analyzed using FlowJo.

### Cell Viability Assays:

To evaluate the cellular cytotoxicity, 20,000 cells in 100 uL media were plated to each well of 96-well plate and incubated them overnight at 37 °C maintaining 5% $CO_2$. Afterwards old media was replaced with new media containing different concentration of antibody/APC as needed. After 30 minutes of incubation, the media was removed, cells were washed with PBS and 100 μL of fresh media was added in each well. After 48 h of additional incubation, 100 μL of CellTitre-Glo (Promega) was added to each well and incubated for 10 minutes with gentle shaking at room temperature. Finally, 100 μL of solutions from each were transferred to opaque white 96 well plate and recorded the luminescence.

## RESULT AND DISCUSSION

### APC was synthesized via strain-promoted azide-alkyne cycloaddition (SPAAC) reaction between DBCO linked antibody and azido terminal polymer:

We chose the trastuzumab (herceptin) antibody targeting human epidermal growth receptor 2 (HER2) and mertansine (DM1) as the drug for the APC construction (Scheme 1). The polymer is designed to offer covalent attachment of the antibody to the chain terminus and reversible covalent attachment of the drug, offering the scaffold's cellular targeting and intracellular drug release capabilities respectively. Conjugation of the polymer to the antibody would be enabled by the azide functionality in the RAFT polymerization, while the pyridyldisulfide-based monomer in the random copolymer chain enables the reversible attachment of the DM1 drug. A PEG-based co-monomer is used to achieve a copolymer of 17.4 kDa molecular weight that offers the opportunity to conjugate multiple drug molecules, while mitigating potential hydrophobicity-based physicochemical instability issues. In comparison to common linker, the higher molecular weight of polymer offers (*i*) higher DAR per single conjugation site on antibody, (*ii*) easy tunability of polymer molecular weight depending on the potency and requirement of drugs, (*iii*) better hydrophobic masking of drug by higher content of hydrophilic pool. Synthesis of the targeted polymer, attachment of DM1 using a simple thiol-disulfide exchange reaction, and conjugation of the polymer to the mAb through an azide-alkyne click chemistry are shown in Scheme 1. Details on the synthesis and characterization of polymers are described in the Supporting Information.

On the antibody side, we used a heterobifunctional PEG molecule (NHS-PEG8-DBCO) to conjugate the DBCO-functionalized linker to the antibody *via* the NHS-lysine reaction.[23] We used the relative absorbances at 310 nm (DBCO) and 280 nm (antibody) to estimate the linkers-to-antibody ratio (LAR) (Figure 2a). Incubation of the antibody with an excess of the heterobifunctional PEG (7 and 45 equivalents) resulted in ~2 and ~5 LAR, respectively, for both anti-HER2 and IgG (isotype control) antibodies (Figure 2b).[24] We then click-conjugated the azide-functionalized polymer to the DBCO-functionalized antibodies. With the LARs of 2 and 5, we formulated two versions of antibody polymer conjugates, $Ab/P_{low}$ and $Ab/P_{high}$ (Figure 2c) respectively. Appearance of a smeared band in SDS-PAGE has been used as an indication for successful protein-polymer conjugation.[25] In our case, we

similarly observed smeared bands in the SDSPAGE gel for Ab/$P_{low}$ and Ab/$P_{high}$ systems for both antibodies (Figure 2d). Similar smeared band in the Western blot for the conjugates further confirms the successful attachment of polymers to antibody (Figure S5a). Since the appearance of DBCO peak intensity at 310 nm provides the LAR information, we sought to use change in this peak intensity upon click reaction as a measure to quantify the number of polymers chains per antibody (Figure S5b). Incubating 20 equivalent polymers per linker in each antibody led to an average of ~1.5 and ~3 polymer chains per antibody for Ab/$P_{low}$ and Ab/$P_{high}$ APC, respectively (Figure S6). After establishing the successful antibody conjugation with free polymer chain, we then constructed the APC with DM1-conjugated polymer following the same method. The DM1 drug was conjugated to the polymer chain via thiol-disulfide exchange reaction (Figure 2e). The distinct absorbance intensity of the reaction byproduct (2-mercaptopyridine) at 343 nm[26] was used to quantify the number of drugs attached per polymer chains (Figure 2f). After that, we have combined the LAR, drugs per polymer chain and SPAAC click percentage to quantitatively determine the DAR (Figure S8, Table 1).

## Flow cytometry assay confirmed the specificity of APCs towards HER2 receptor:

Following the DAR calculation of APCs, we evaluated the binding interactions using a flow assay in HER2+ SKOV3 cells.[27] To evaluate the possible loss in targeting ability of the antibody due to the polymer conjugation, we first used a fluorophore-tagged secondary antibody that binds to the Fc domain of primary antibody on cell surface (Figure 3a). The specificity in binding would then be discerned from the fluorescence intensity differences achieved from the anti-HER2 Ab and the control IgG Ab. Indeed, we observed higher MFI for both anti-HER2/$P_{low}$ and anti-HER2/$P_{high}$ constructs in HER2+ cells (SKOV3) relative to the HER2- cells (MCF10A) (Figure 3b, 3c). Similarly, we also tested the binding of IgG/$P_{low}$ and IgG/$P_{high}$ control systems in both cell lines. Neither of the systems showed any significant binding to either of the cell lines (SKOV3 or MCF10A), demonstrating the specific binding of the anti-HER2-based APCs towards the HER2+ cell line. Moreover, we further confirmed the specificity of APCs alternatively by conjugating a fluorophore (sulfonated-Cy3) tagged polymer P2 to anti-HER2 antibody (Figure 3d, 3e).[26] Flow cytometric evaluation of these fluorophore-conjugated APC scaffolds further support their binding specificity (Figure 3f).

## HER2 APC showed receptor specific cell killing and is more potent than ADC (Kadcyla®) in HER2+ cells:

Next, we tested cell killing profile of APCs and compared the efficacy with the corresponding ADC in the clinic, Kadcyla®. The cytotoxicity profile of free antibodies (both anti-HER2 and isotype IgG) and the respective APCs (APC/$P_{low}$ and APC/$P_{high}$) were first evaluated in MCF10A cells, a HER2- cell line, using the CellTiter-Glo luminescent cell viability assay. As shown in Figure 4a, neither the free antibodies nor any formats of the APCs (anti-HER2 or isotype IgG) showed any cytotoxicity in MCF10A cells. Cytotoxicity of all these constructs were then evaluated in HER2+ cell line, SKOV3 cells. Free antibodies (anti-HER2 and isotype IgG) were found to be non-toxic, and the APCs based on IgG showed minimal cytotoxicity and that too at higher concentrations (Figure 4b). On the other hand, both HER2/APC-$P_{low}$ and HER2/APC-$P_{high}$ lead to ~40% cell killing in SKOV3

cell lines (Figure 4b). Though we observe an epitope-dependent selective cytotoxicity with HER2/APCs, we were concerned about the observed saturation in their cell kill. We varied a few conditions, including increasing DAR, repeat dosing, with the hopes of improving the cytotoxicity profiles. Improvement only got up to ~60% cell kill for high DAR constructs (Figure S12). We then tested the cytotoxicity of the free DM1 drug in both SKOV3 and MCF10A cells (Figure S13). While very effective in MCF10A cell kill, a saturation was observed in SKOV3 cells even with the free drug. These results indicate a possible latent drug resistance for DM1 drug in SKVO3 cells.

Then we tested the cytotoxicity in other cell lines with higher HER2 receptor expression as it would possibly increase the engagement of more APC on cell surface. To test the broad applicability of the APC strategy, the anti-HER2 formulations were tested in SKBR3 and BT474 cell lines which have been reported to have high HER2 receptor expression. First, we assessed the relative HER2 receptor expression levels of all four cell lines using a fluorophore tagged HER2 antibody via flow cytometry (Figure 4c). Then we tested the specific binding interaction of APC/$P_{high}$ in both SKBR3 (Figure 4d) and BT747 (Figure S14b) cells. Once the specificity was established in both of these HER2+ cells, we tested cytotoxicity of HER2/$APC_{high}$ in these cells using CellTiter-Glo assay. While free antibodies remained nontoxic in both cell lines (Figure S15), HER2/$APC_{high}$ exhibits significant cytotoxicity to SKBR3 and BT474 cells. Even though the HER2 receptor expression in BT474 is higher than the SKOV3 cells, HER2/$APC_{high}$ exhibits much poorer cell killing in BT474 cells (Figure S16b). This could be attributed to the inherent resistance of specific cells to the cytotoxic DM1, which is supported by the lower cell killing efficiency of free DM1 drug in BT474 cells (Figure S13c). Three key features attest to the specificity offered by the APC scaffold: (i) the degree of cell kill by the APC scaffolds in HER2+ cells are similar to those observed for both the free drug DM1 and are even better than the corresponding clinically used ADC (Figure 4e, Figure S16a, Figure S17); (ii) although there is a high degree of cell kill by the free drug DM1 in the HER2- (MCF10A) cells, the cell kill is much lesser for the HER2/APCs (Figure 4a, Figure S13a); (iii) IgG/APCs remained nontoxic across all cells tested with negligible toxicities only at higher concentrations (Figure 4a & 4b, Figure S18).

### APCs can be strategically engineered to accommodate desired drugs of interest:

DM1 has a thiol functionality that is conveniently used for functionalizing the polymer attached to the antibody. If this were a pre-requisite, then the platform outlined here would be quite limited. To test the versatility of this approach to accommodate different payloads, we were interested in testing the modularity of the system in terms of its potential to accommodate variations in the drug molecule and the antibody. To this end, we designed another polymer **(Polymer P3)** (Figure S20) with an activated carbonate functionality that can serve as the handle to conjugate payloads containing hydroxyl or amine moieties (Figure 5a).[28,29] Additionally, the disulfide bond at the beta position to the resultant carbonate (or carbamate) in the polymer side chain is designed to be self-immolative nature in the presence of endogenous stimuli, such as intracellular GSH, to release the payload in its active form. To demonstrate this, we chose SN38 as a payload which is a topoisomerase inhibitor irinotecan metabolite.[30] The recent FDA approval of Trodelvy® (Sactiuzumab

govitecan) ADC for triple-negative breast cancer (TNBC) attests to the value of SN38 in the clinic.[31] We conjugated SN38 to the polymer and quantified the conjugation percentage (~56%) using the UV-vis absorbance peak at 333 nm, corresponding to the release of p-nitrophenol (Figure 5b) (Figure S21). Then we calculated the number of polymer drugs per polymer chain to estimate the DAR of the system (Table S3). Finally, we evaluated the cytotoxicity of SN38 based APC system in SKOV3 cell (Figure 5c) which showed selective cell killing of HER2/$SN38_{high}$ while the IgG/APC (control) remained non-toxic (Figure 5d). The result obtained not only reassured the selectivity in cell killing, but it also demonstrates the broader applicability of the APC platform.

### Altering the targeting antibody to anti-EGFR was equally effective in selectively killing EGFR+ cells and shows the flexibility in antibody choice for APC:

Finally, we further demonstrated the broad utility of the platform using another disease relevant antibody. For this, we chose epidermal growth factor receptor (EGFR) as a target, as it is reported to be one of the frequently overexpressed target epitopes for triple-negative breast cancer (TNBC).[21] We used same linker equivalent and conjugation condition methods to obtain the desired LAR in anti-EGFR antibody and the corresponding APC (Figure 6a and 6b). We also confirmed the specific binding of EGFR/$P_{high}$ in A431 cells (EGFR+) using the secondary antibody assay using flow cytometry (Figure 6c, 3a). Finally, we evaluated the toxicity of free drug (DM1) and EGFR/APC, where we observed the specific cell killing of A431 cells, relative to the corresponding IgG control (Figure 6d, 6e). The higher toxicity of EGFR/APC demonstrate the potential for translating the conjugation protocols broadly to different antibodies and drug molecules.

## CONCLUSIONS

In conclusion, we have demonstrated a modular APC platform for the active targeted delivery of chemotherapeutic drugs. We use a simple polymeric extension strategy to: (a) increase the DAR without sacrificing the specificity of antibody towards respective receptors, and (b) use the hydrophilic co-monomer in the polymeric chain to mask the increased hydrophobicity caused by the higher therapeutic payloads attached to the polymer. APCs are formulated via a facile DBCO-azide bioconjugation chemistry. We have demonstrated the specific binding ability and selective cell killing of this platform in multiple HER2+ cell lines. These scaffolds exhibit better cell killing efficacy than the corresponding clinically used ADC, Kadcyla. We also demonstrate the versatility of the modular platform through the use of alternate functional groups that could be used for attaching the drug molecules and antibodies that could be used for cellular targeting. Overall, the APC platform offers a ‘simple yet effective’ way to leverage polymers for the antibody-based active targeted chemotherapeutics delivery.

## Supplementary Material

Refer to Web version on PubMed Central for supplementary material.

## ACKNOWLEDGEMENT

The authors thank the NIGMS (GM-136395) of the NIH for the support. Authors also thank Dr. Kingshuk Dutta for helpful discussions and suggestion with the experiments. The authors appreciate Dr. Amy Burnside in UMass Flow Cytometry facility for experiment suggestions.

### FUNDING SOURCE

We thank NIGMS (GM-136395) of the NIH for the support.

## REFERENCES

1. do Pazo C; Nawaz K; Webster RM The Oncology Market for Antibody-Drug Conjugates. Nat. Rev. Drug Discovery 2021, 20, 583–584. [PubMed: 33762691]
2. Fu Z; Li S; Han S; Shi C; Zhang Y. Antibody Drug Conjugate: The “Biological Missile” for Targeted Cancer Therapy. Signal Transduction Targeted Ther. 2022, 7, 93.
3. Manzari MT; Shamay Y; Kiguchi H; Rosen N; Scaltriti M; Heller DA Targeted Drug Delivery Strategies for Precision Medicines. Nat. Rev. Mater. 2021, 6, 351–370. [PubMed: 34950512]
4. Mullard A. FDA Approves 100th Monoclonal Antibody Product. Nat. Rev. Drug Discovery 2022, 20, 491–495.
5. Tong JT; Harris PW; Brimble MA; Kavianinia I. An Insight into FDA Approved Antibody-Drug Conjugates for Cancer Therapy. Molecules 2021, 26, 5847. [PubMed: 34641391]
6. Teicher BA; Chari RVJ Antibody Conjugate Therapeutics: Challenges and Potential. Clin. Cancer Res. 2011, 17, 6389–6397. [PubMed: 22003066]
7. Khongorzul P; Ling CJ; Khan FU; Ihsan AU; Zhang J. Antibody-Drug Conjugates: A Comprehensive Review. Mol. Cancer Res. 2020, 18, 3–19. [PubMed: 31659006]
8. Baron J; Wang ES Gemtuzumab Ozogamicin for the Treatment of Acute Myeloid Leukemia. Expert Rev. Clin. Pharmacol. 2018, 11, 549–559. [PubMed: 29787320]
9. Drago JZ; Modi S; Chandarlapaty S. Unlocking the Potential of Antibody–Drug Conjugates for Cancer Therapy. Nat. Rev. Clin. Oncol. 2021, 18, 327–344. [PubMed: 33558752]
10. Gordon MR; Canakci M; Li L; Zhuang J; Osborne B; Thayumanavan S. Field Guide to Challenges and Opportunities in Antibody-Drug Conjugates for Chemists. Bioconjugate Chem. 2015, 26, 2198–2215.
11. Beck A; Goetsch L; Dumontet C; Corvaïa N. Strategies and Challenges for the Next Generation of Antibody-Drug Conjugates. Nat. Rev. Drug Discovery 2017, 16, 315–337. [PubMed: 28303026]
12. Polakis P. Antibody Drug Conjugates for Cancer Therapy. Pharmacol. Rev. 2016, 68, 3–19 [PubMed: 26589413]
13. Hamblett KJ; Senter PD; Chace DF; Sun MMC; Lenox J; Cerveny CG; Kissler KM; Bernhardt SX; Kopcha AK; Zabinski RF; Meyer DL; Francisco JA Effects of Drug Loading on the Antitumor Activity of a Monoclonal Antibody Drug Conjugate. Clin. Cancer Res. 2004, 10, 7063–7070. [PubMed: 15501986]
14. Sun X; Ponte JF; Yoder NC; Laleau R; Coccia J; Lanieri L; Qiu Q; Wu R; Hong E; Bogalhas M. Effects of Drug-Antibody Ratio on Pharmacokinetics, Biodistribution, Efficacy, and Tolerability of Antibody-Maytansinoid Conjugates. Bioconjugate Chem. 2017, 28, 1371–1381.
15. Jeffrey SC; Andreyka JB; Bernhardt SX; Kissler KM; Kline T; Lenox JS; Moser RF; Nguyen MT; Okeley NM; Stone IJ; Zhang X; Senter PD Development and Properties of Beta-Glucuronide Linkers for Monoclonal Antibody-Drug Conjugates. Bioconjugate Chem. 2006, 17, 831–840.
16. Moon S-J; Govindan SV; Cardillo TM; D’Souza CA; Hansen HJ; Goldenberg DM Antibody Conjugates of 7-ethyl-10-hydroxycamptothecin (SN-38) for Targeted Cancer Chemotherapy. J. Med. Chem. 2008, 51, 6916–6926. [PubMed: 18939816]
17. Tedeschini T; Campara B; Grigoletto A; Bellini M; Salvalaio M; Matsuno Y; Suzuki A; Yoshioka H; Pasut G. Polyethylene Glycol-based Linkers as Hydrophilicity Reservoir for Antibody-Drug Conjugates. J. Controlled Release 2021, 337, 431–447.

18. Forsythe NL; Tan MF; Maynard HD Diazido Macrocyclic Sulfates as a Platform for the Synthesis of Sequence-Defined Polymers for Antibody Drug Conjugates. Chem. Sci. 2022, 13, 3888–3893. [PubMed: 35432892]
19. Lyon RP; Bovee TD; Doronina SO; Burke PJ; Hunter JH; Neff-LaFord HD; Jonas M; Anderson ME; Setter JR; Senter PD Reducing Hydrophobicity of Homogeneous Antibody-Drug Conjugates Improves Pharmacokinetics and Therapeutic Index. Nat. Biotechnol. 2015, 33, 733–735. [PubMed: 26076429]
20. Amiri-Kordestani L; Blumenthal GM; Xu QC; Zhang L; Tang SW; Ha L; Weinberg WC; Chi B; Candau-Chacon R; Hughes P; Russell AM; Miksinski SP; Chen XH; McGuinn WD; Palmby T; Schrieber SJ; Liu Q; Wang J; Song P; Mehrotra N; Skarupa L; Clouse K; Al-Hakim A; Sridhara R; Ibrahim A; Justice R; Pazdur R; Cortazar P. FDA Approval: Ado-Trastuzumab Emtansine for the Treatment of Patients with HER2-Positive Metastatic Breast Cancer. Clin. Cancer Res. 2014, 20, 4436–4441. [PubMed: 24879797]
21. Nakai K; Hung MC; Yamaguchi H. A Perspective on Anti-EGFR Therapies Targeting Triple-Negative Breast Cancer. Am. J. Cancer Res. 2016, 6, 1609–1623. [PubMed: 27648353]
22. Singh K; Canakci M; Kanjilal P; Williams N; Shanthalingam S; Osborne BA; Thayumanavan S. Evaluation of Cellular Targeting by Fab′ vs Full-Length Antibodies in Antibody-Nanoparticle Conjugates (ANCs) Using CD4 T-cells. Bioconjugate Chem. 2022, 33, 486–495.
23. Canakci M; Singh K; Munkhbat O; Shanthalingam S; Mitra A; Gordon M; Osborne BA; Thayumanavan S. Targeting CD4+ cells with Anti-CD4 Conjugated Mertansine-Loaded Nanogels. Biomacromolecules 2020, 21, 2473–2481 [PubMed: 32383874]
24. Pelegri-O'Day EM; Matsumoto NM; Tamshen K; Raftery ED; Lau UY; Maynard HD PEG Analogs Synthesized by Ring-Opening Metathesis Polymerization for Reversible Bioconjugation. Bioconjugate Chem. 2018, 29, 3739–3745.
25. Kanjilal P; Dutta K; Thayumanavan S. Thiol-Disulfide Exchange as a Route for Endosomal Escape of Polymeric Nanoparticles. Angew. Chem., Int. Ed. 2022, 61, e202209227.
26. Huynh U; Wu P; Qiu J; Prachyathipsakul T; Singh K; Jerry DJ; Gao J; Thayumanavan S. Targeted Drug Delivery Using a Plug-to-Direct Antibody-Nanogel Conjugate. Biomacromolecules 2023, 24, 849–857 [PubMed: 36639133]
27. Dutta K; Kanjilal P; Das R; Thayumanavan S. Synergistic Interplay of Covalent and Non-Covalent Interactions in Reactive Polymer Nanoassembly Facilitates Intracellular Delivery of Antibodies. Angew. Chem., Int. Ed. 2021, 133, 1849–1858.
28. Dutta K; Hu D; Zhao B; Ribbe AE; Zhuang J; Thayumanavan S. Templated Self-Assembly of a Covalent Polymer Network for Intracellular Protein Delivery and Traceless Release. J. Am. Chem. Soc. 2017, 139, 5676–5679. [PubMed: 28406017]
29. Maurya D; Ayuzawa R; Doi C; Troyer D; Tamura M. Topoisomerase I inhibitor SN-38 Effectively Attenuates Growth of Human Non-Small Cell Lung Cancer Cell Lines In Vitro and In Vivo. J. Environ. Pathol., Toxicol. Oncol. 2011, 30, 1–10. [PubMed: 21609311]
30. Guerra E; Alberti S. The Anti-Trop-2 Antibody-Drug Conjugate Sacituzumab Govitecan-Effectiveness, Pitfalls and Promises. Ann. Transl. Med. 2022, 10, 501. [PubMed: 35928735]

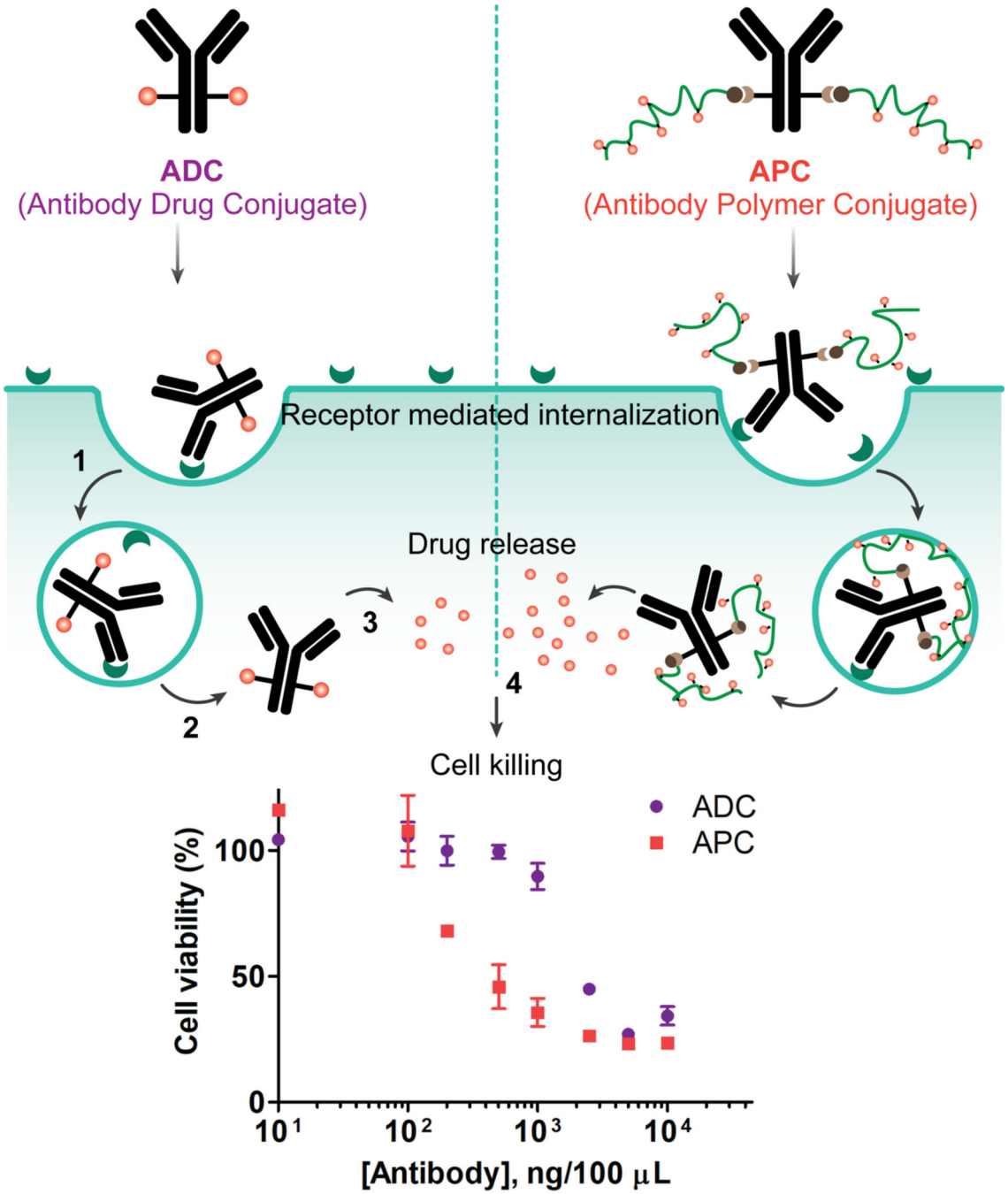


**Figure 1:**

Schematic illustration of the proposed hypothesis on the advantages of APC over ADC. Both constructs bind to the cell surface antigen (1) and can be internalized via receptor mediated endocytosis[9] (2). The cytotoxic payload is released in the cytosol (3) which induces cell death (4). APCs have high and tunable DAR and showed improved efficacy ($IC_{50}$) in compared to commercially available ADC. The inset figure represents the comparative cytotoxicity of APC and ADC in SKBR3 (HER2+) cells.

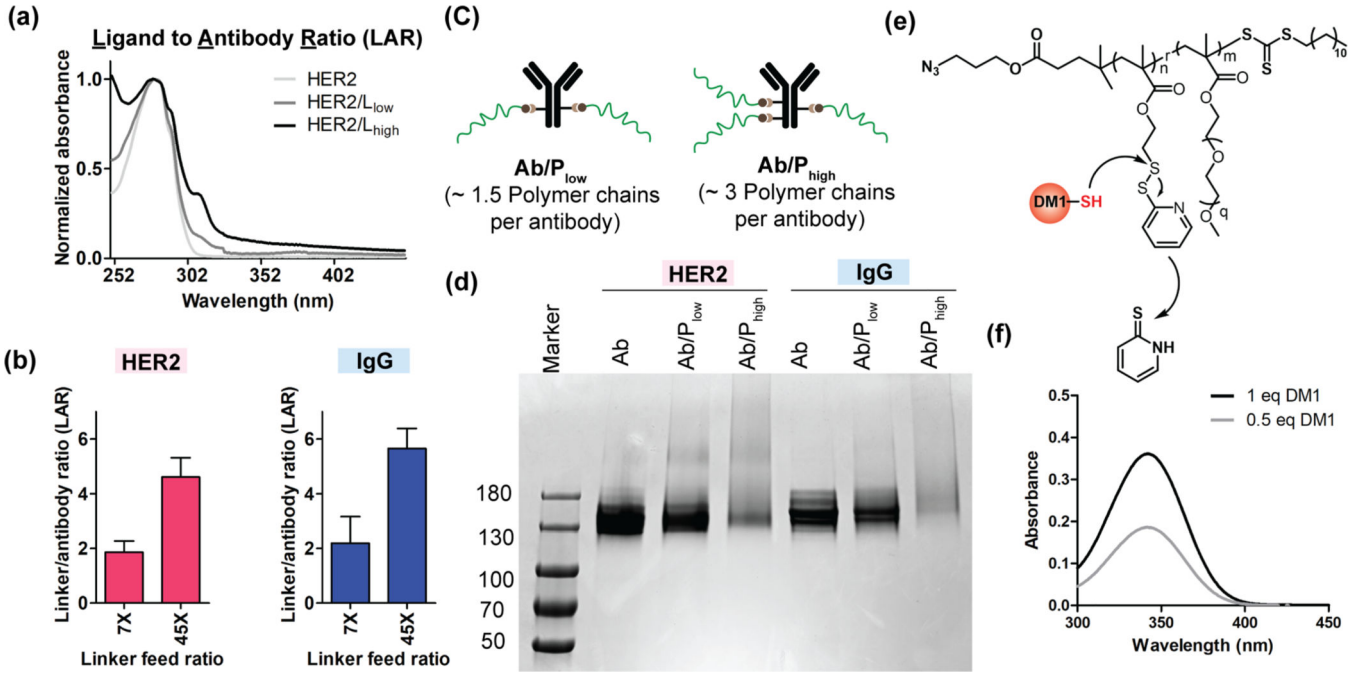


**Figure 2:**

Confirmation of antibody polymer conjugation and calculation of DAR. **(a)** UV-vis spectrum of linker conjugated antibody was used to determine the linker to antibody ratio (LAR). The ratio of absorbance at 310 nm (DBCO) and absorbance at 280 nm (antibody) was used to determine the LAR. **(b)** Optimized LAR of anti-HER2 and IgG (isotype control) antibodies at 7X and 45X feed ratio. **(c)** Representation of two antibody polymer (free polymer) conjugate system studied in this work. The number of polymer chains in each system represents the ratio of obtained number of polymers per antibody. **(d)** Gel electrophoresis image of antibody polymer (free polymer) conjugates for both HER2 and IgG antibodies. The tailing nature of bands for $Ab/P_{high}$ for both HER2 and IgG confirms the higher number of polymer conjugations to antibody. **(e)** The reaction scheme of DM1 drug conjugation to polymer chains via thiol-disulfide exchange reactions. **(f)** UV-vis spectrum of released byproduct (2-mercaptopyridine) from polymer chain after drug conjugation reaction. The concentration of 2-mercaptopyridine was used to determine the number drugs per polymer chains.

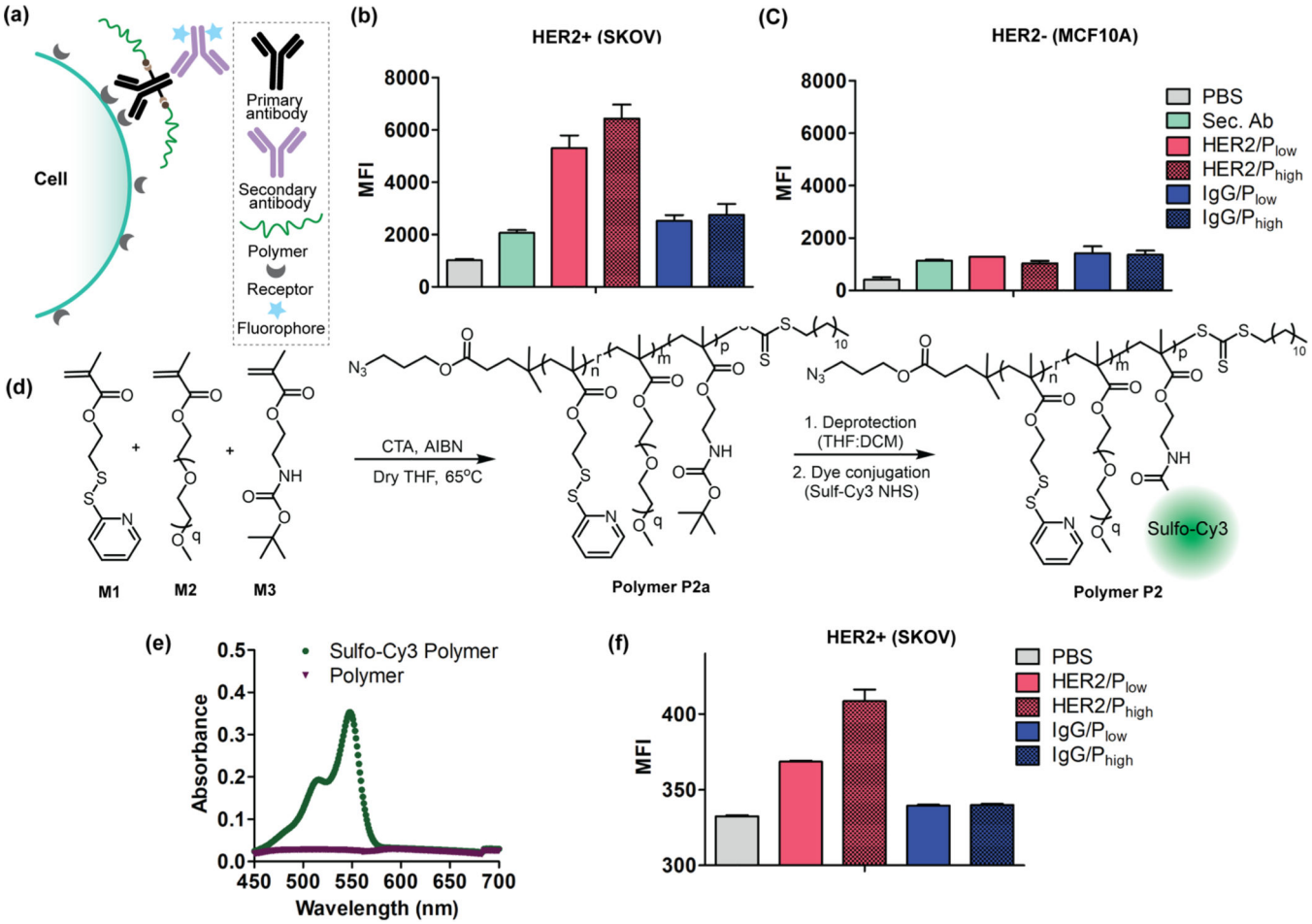


**Figure 3:**

Evaluation of specificity of APCs towards HER2 receptors. **(a)** Schematic representation of APC binding interaction evaluation using fluorophore-labeled secondary antibody. Specificity evaluation of HER2/APCs and IgG/APCs (control) in **(b)** SKOV cells (HER2+) and **(c)** MCF10A (HER2-) cells; Sec. Ab: Secondary Antibody. **(d)** Synthetic scheme of polymer **P2** conjugation with fluorophore (Sulfo-Cy3 NHS). **(e)** UV-vis spectrum of dye tagged polymer with an absorbance maximum at 548 nm confirming the successful conjugation of dye to the polymer. **(f)** The dye tagged polymer was conjugated to antibodies (anti-HER2 and IgG) and studies the binding specificity of APCs in SKOV3 cell (HER2+) using flow cytometry.

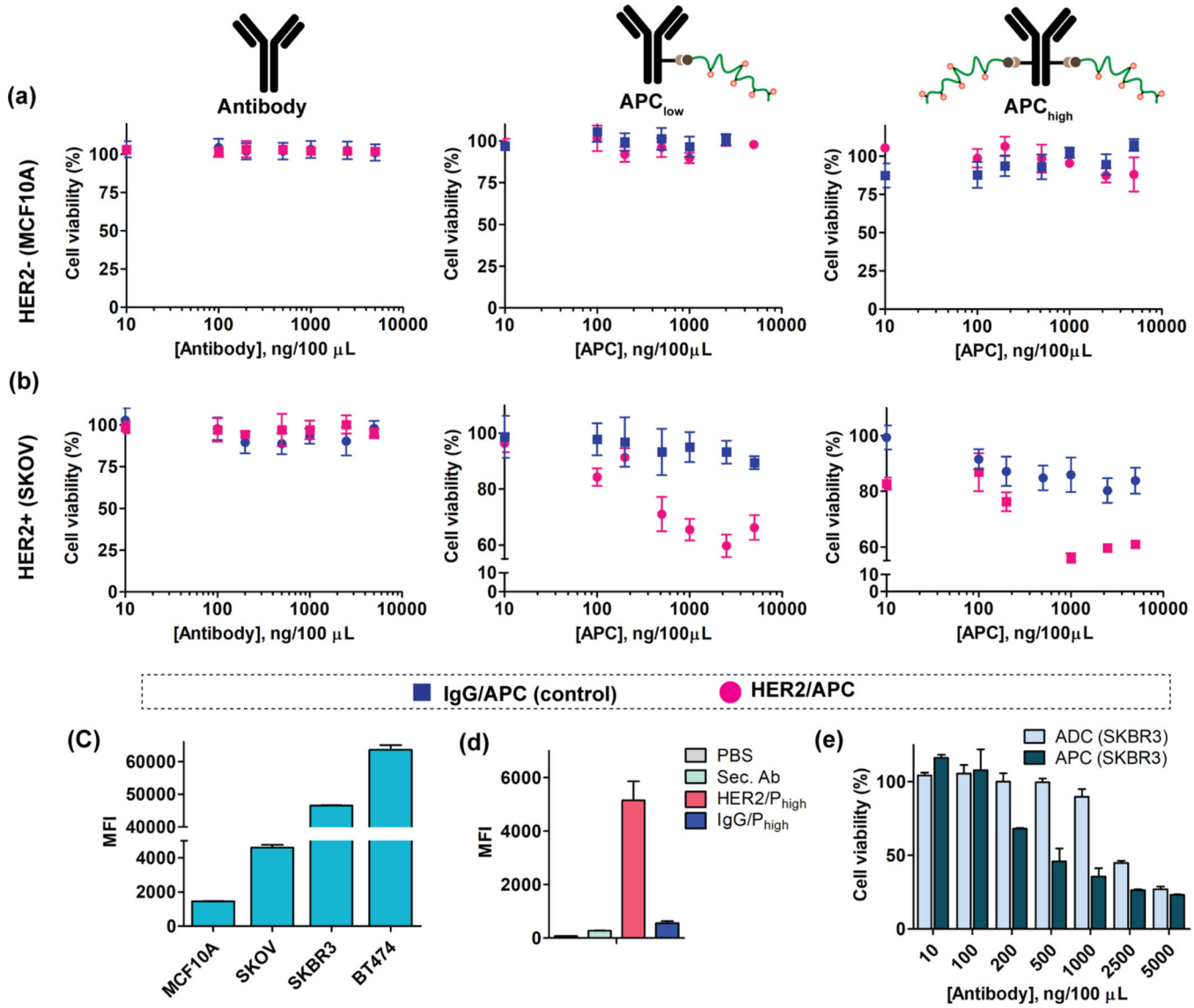


**Figure 4:**

Cytotoxicity evaluation of APCs in HER2+/− cells. **(a)** The cell viability of free antibody (both HER2 and IgG), comparative cytotoxicity of APC-P$_{low}$ and APC-P$_{high}$ in MCF10A (HER2-) cells. **(b)** The cell viability of free antibody (both HER2 and IgG), comparative cytotoxicity of APC/P$_{low}$ and APC/P$_{high}$ in SKOV3 (HER2+) cells. **(c)** Receptor expression quantification of HER2 in four different cell lines. **(d)** Specificity evaluation of APCs in SKBR3 cell using dye tagged secondary antibody. **(e)** Comparative cytotoxicity study of HER2/APC with Kadcyla® ADC in SKBR3 (HER2+) cell.

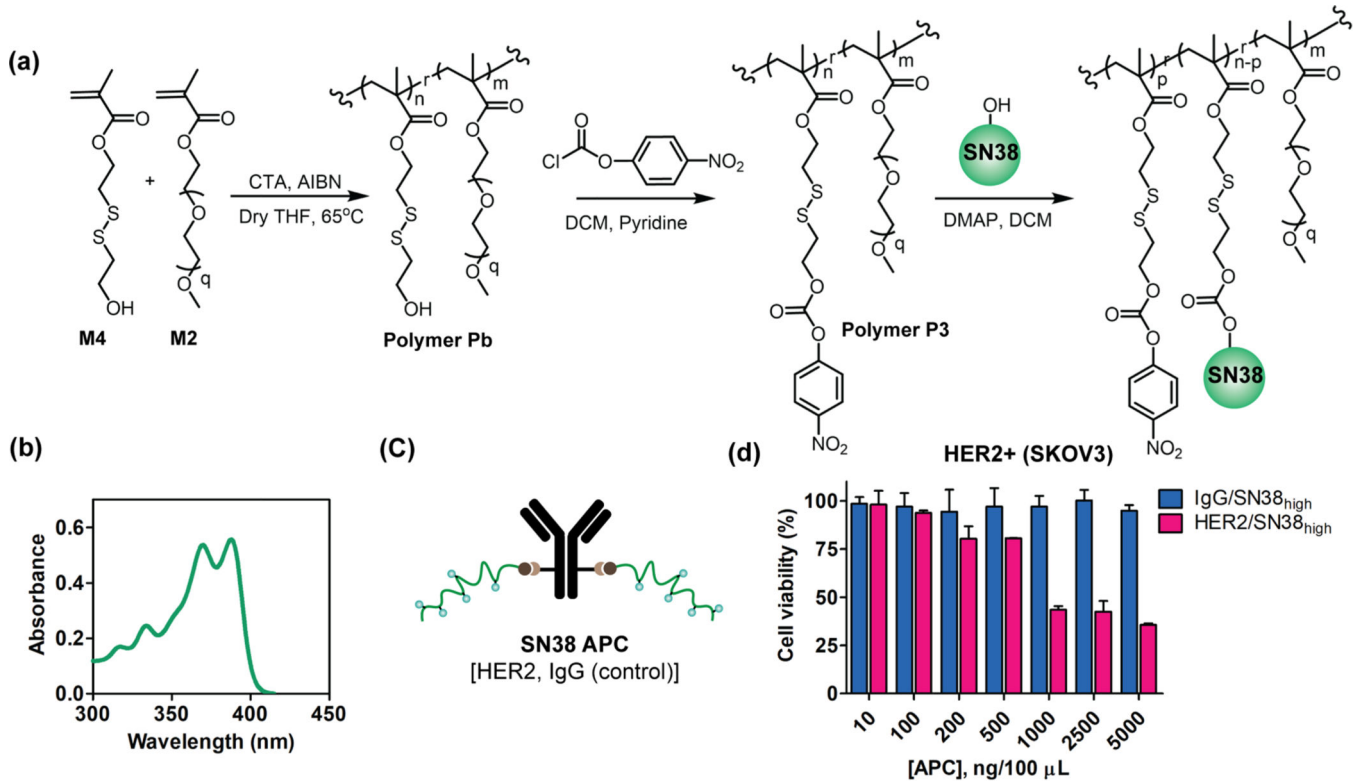


**Figure 5:**

Synthesis and cytotoxicity studies of HER2/APC with SN38 (7-ethyl-10-hydroxycampothecin) drug. **(a)** Total synthetic scheme of polymer **P3** and SN38 conjugation reaction. **(b)** UV-vis absorbance of drug conjugated polymer. The absorbance peak at 370 nm confirms the conjugation of drug to the polymer. **(c)** SN38 HER2/APC construct. **(d)** Cytotoxicity evaluation of HER2/$SN38_{high}$ and IgG/$SN38_{high}$ in SKOV3 (HER2+) cell.

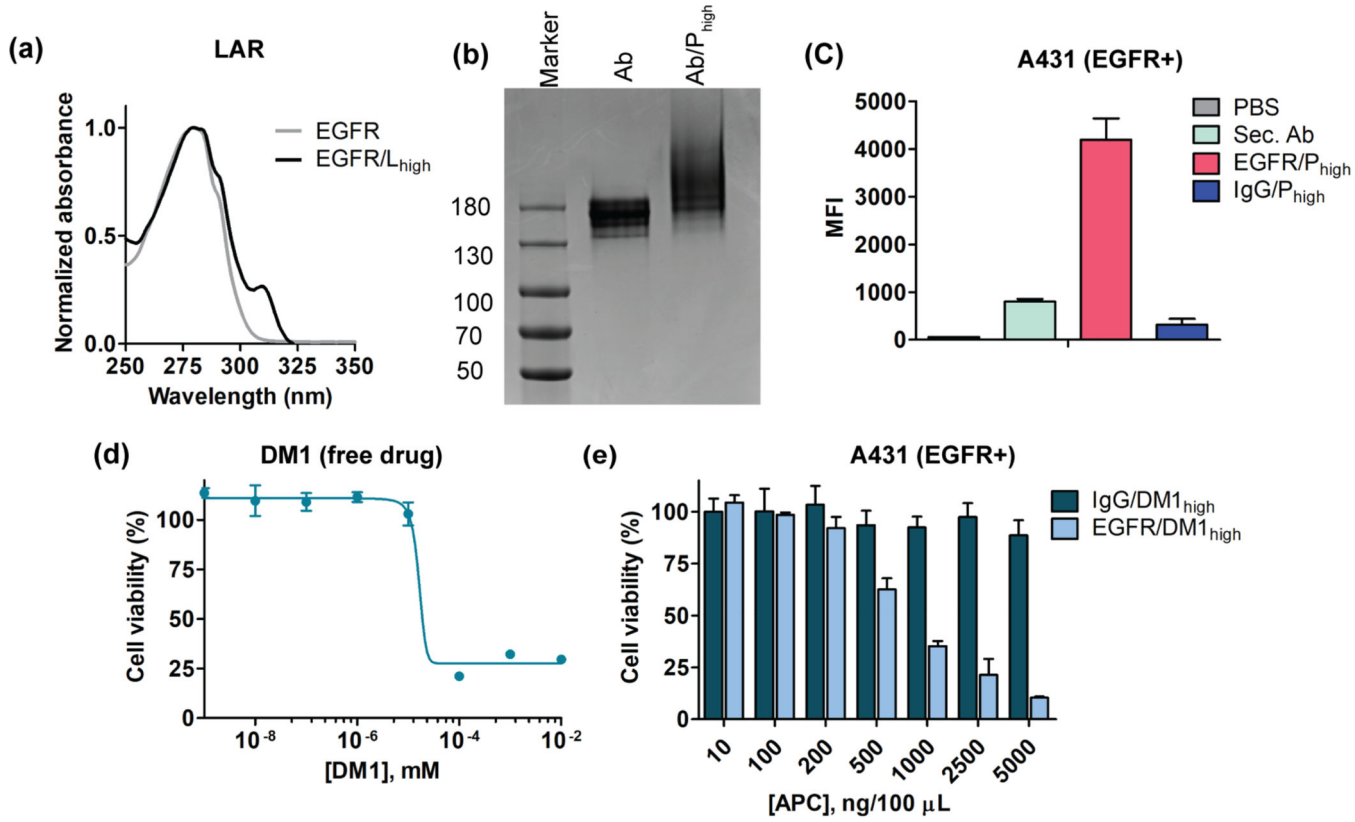


**Figure 6:**

Specificity and cytotoxicity studies of EGFR/APC with DM1 drug. **(a)** UV-vis spectrum of EGFR antibody linker conjugates. The absorbance at 310nm confirms the successful conjugation of linker to the antibody. **(b)** Gel electrophoresis of Ab (free antibody) and Ab-$P_{high}$ (EGFR/APC). The smeared elongation in case of Ab-$P_{high}$ confirms polymer conjugation to antibody. **(c)** Specificity studies of EGFR/APC in A431 cell (EGFR+). **(d)** Free drug toxicity of DM1 in A431 cell. **(e)** Cytotoxicity evaluation of EGFR/$APC_{high}$ and IgG/$APC_{high}$ in A431 (EGFR+) cell.

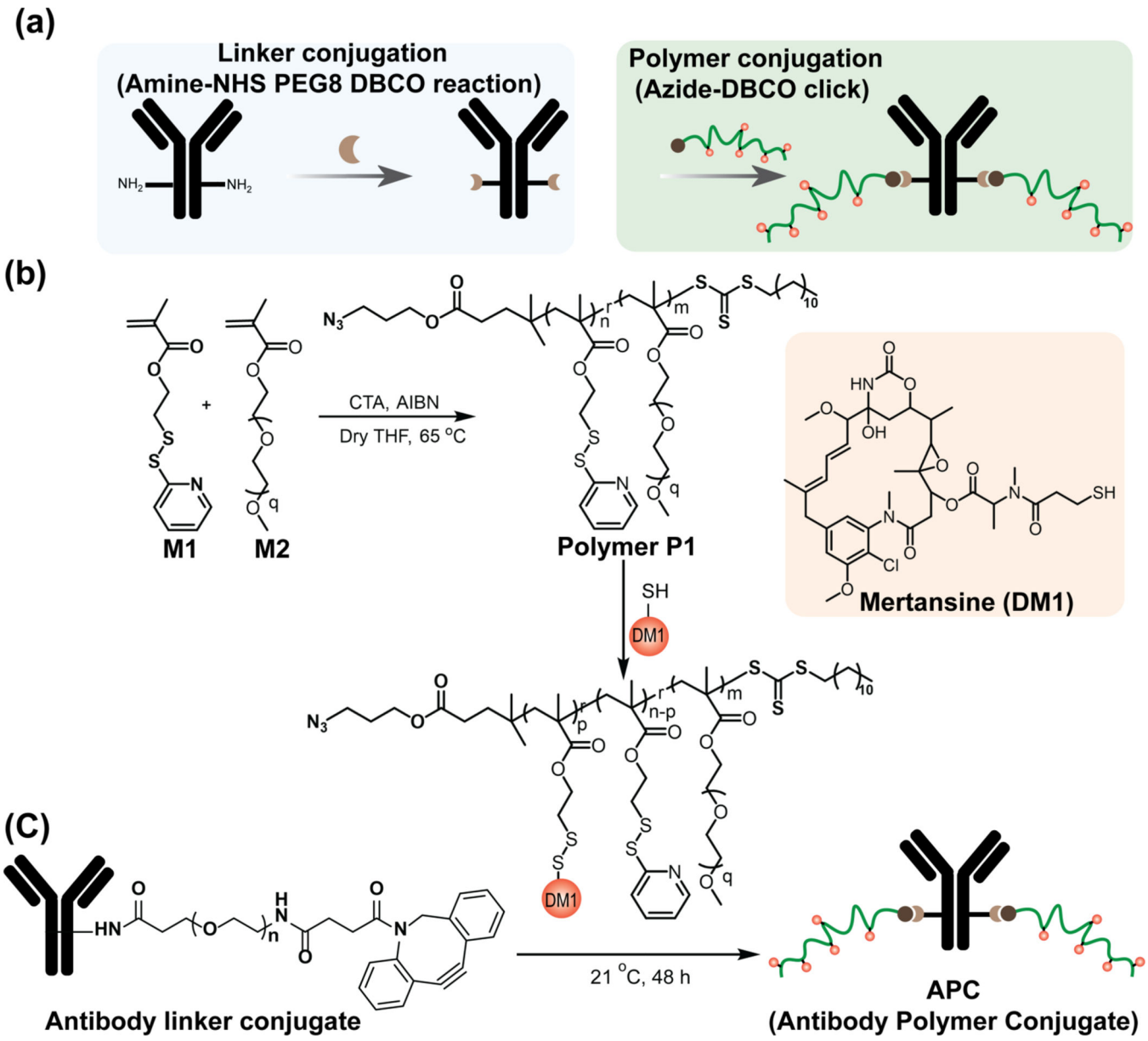


**Scheme 1:**

Synthetic reaction scheme for APC. **(a)** Total synthetic scheme of APC starting with linker conjugation to antibody, followed by polymer conjugation. Linker was conjugated to antibody using Amine-NHS chemistry between antibody lysine and NHS-PEG8-DBCO linker. Later, DBCO-Azide click chemistry was employed to conjugate polymers to the antibody. The polymer chains are randomly conjugated to the antibody using surface lysine functionalities **(b)** Synthetic scheme of drug conjugated polymer. Polymer was synthesized using RAFT polymerization technique and drug was conjugated to the polymer using thiol-disulfide exchange reactions. **(c)** The polymer conjugation to antibody via azide-DBCO click chemistry.

**Table 1:**

The table summarizes the calculated DAR of APCs for DM1 drug.

| | **0.5 eq DM1 (polymer P1)** | | **1 eq of DM1 (polymer P1)** | |
|---|---|---|---|---|
| | **Ab/$P_{low}$** | **Ab/$P_{high}$** | **Ab/$P_{low}$** | **Ab/$P_{high}$** |
| HER2/APC | 8.46 | 15.07 | 17.12 | 30.49 |
| IgG/APC | 9.31 | 17.03 | 18.83 | 34.45 |